Sequential-Pulse Laser-Induced Breakdown Spectroscopy of High-Pressure Bulk Aqueous Solutions

MARION LAWRENCE-SNYDER, JON SCAFFIDI, S. MICHAEL ANGEL,* ANNA P. M. MICHEL, and ALAN D. CHAVE

Department of Chemistry and Biochemistry, University of South Carolina, Columbia, South Carolina 29208 (M.L.S., J.S., S.M.A.); Massachusetts Institute of Technology/Woods Hole Oceanographic Institution Joint Program Department of Applied Ocean Physics and Engineering, Woods Hole Oceanographic Institution, MS#7, Woods Hole, Massachusetts 02543 (A.P.M.M.); and Department of Applied Ocean Physics and Engineering, Woods Hole Oceanographic Institution, MS#7, Woods Hole, Massachusetts 02543 (A.D.C.)

Sequential-pulse (or dual-pulse) laser-induced breakdown spectroscopy (DP-LIBS) with an orthogonal spark orientation is described for elemental analysis of bulk aqueous solutions at pressures up to ~138 × 10^5 Pa (138 bar). The use of sequential laser pulses for excitation, when compared to single-pulse LIBS excitation (SP-LIBS), provides significant emission intensity enhancements for a wide range of elements in bulk solution and allows additional elements to be measured using LIBS. Our current investigations of high-pressure solutions reveal that increasing solution pressure leads to a significant decrease in DP-LIBS emission enhancements for all elements examined, such that we see little or no emission enhancements for pressures above 100 bar. Observed pressure effects on DP-LIBS enhancements are thought to result from pressure effects on the laser-induced bubble formed by the first laser pulse. These results provide insight into the feasibility and limitations of DP-LIBS for *in situ* multi-elemental detection in high-pressure aqueous environments like the deep ocean.

Index Headings: **Laser-induced breakdown spectroscopy; LIBS; Sequential-pulse; Dual-pulse; Plasma; High pressure; Bulk solution.**

INTRODUCTION

Laser-induced breakdown spectroscopy (LIBS), first reported by Brech and Cross in 1962,[1] is a relatively simple spectroscopic technique that has the potential to provide sustained, *in situ*, multi-elemental detection in high-pressure aqueous environments like the deep ocean. Besides having the ability to rapidly analyze the elemental composition of solids, liquids, and gases with little or no sample preparation, LIBS is one of the few techniques capable of non-contact and remote elemental analysis,[2–20] making it particularly useful for analyses in extreme and hostile environments such as those found in the deep ocean.[10–18,21–31]

Despite the obvious potential of LIBS for oceanographic applications, there has been very little research examining LIBS analyses of bulk aqueous solution, with most work limited to atmospheric-pressure solutions.[32–49] This limited attention may in part be attributed to the difficulties associated with LIBS analysis in bulk liquids using a single laser pulse (SP-LIBS), including reduced laser-induced plasma (LIP) emission intensity due to strong plasma quenching by the dense liquid matrix (much of the plasma energy goes into vaporization of the liquid)[36,37,44–47] and increased broadening of atomic emission lines associated with elevated collisional broadening and Stark broadening effects.[27,35–37,43–46] Additionally, the speed of electron–ion recombination and rapid plasma cooling in bulk aqueous solution limit the plasma lifetime (typically ~1 μs or less in bulk solution[32,37,38,44–46] versus tens of microseconds in air[37,44,50–52]) such that only emission lines with low-energy excited states are typically detected. For these reasons, hydrogen, oxygen, and many analytes important in ocean chemistry (e.g., Fe, Zn, Cu, Pb, Si, Cl, Br) are very difficult to detect in bulk solution using SP-LIBS.[31,35,38,41]

In 1984, Cremers, et al.[35] demonstrated that the use of sequential laser pulse excitation (often referred to as sequential- or dual-pulse LIBS, DP-LIBS) can provide significant emission intensity enhancements relative to SP-LIBS for metals and ions in bulk aqueous solution, thus providing lower limits of detection and allowing a wider range of elements to be detected. The DP-LIBS emission enhancements are achieved through excitation of a gaseous cavity or vapor bubble formed by laser-induced dielectric breakdown of the solution by the first LIP.[34–37,44,47–49,52] In general, the high plasma temperatures and pressures (6000–15 000 K and 20–60 kbar, respectively)[32] generated upon formation of the first LIP cause thermal expansion of the plasma and consequent formation of a vapor bubble or cavity (i.e., a thin layer of vapor and diffused gas) around the plasma volume. As the ultra-hot plasma heats the gaseous cavity, the pressure inside the bubble rapidly increases, causing the bubble wall to expand.[32] The volume of the laser-induced bubble continues to grow until the pressure inside the bubble falls below that of the surrounding liquid, at which point the bubble begins to shrink, often oscillating several times before collapsing. While emission resulting from a LIP formed in bulk solution or in a laser-induced bubble often ceases within several microseconds, the laser-induced bubble oscillation period (expansion to collapse) has been shown to have a lifetime (in atmospheric-pressure solutions) on the order of a hundred microseconds.[32,37,41,44,49,53]

When the second LIP is focused inside the laser-induced vapor bubble, the resulting emission more closely resembles that produced by a single LIP in air, as compared to a LIP formed in bulk solution.[35,37,44,45] As a result, the rapid rate of quenching associated with SP-LIBS in bulk solution slows considerably. Since Cremers' initial report,[35] several groups have successfully used DP-LIBS for in-bulk analysis of aqueous solutions,[34,35,41,44,47,48,54] but to the best of our knowledge we are the first research group to examine SP- and DP-LIBS in a high-pressure aqueous environment.[31,55]

In previous work, we reported the first high-pressure SP-LIBS measurements of a range of elements (Na, Ca, Li, K, and Mn) in bulk aqueous solution at pressures exceeding 276 bar.[31] We also demonstrated that solution pressure has little effect on SP-LIBS emission intensities and peak widths. As expected, easily ionized elements were readily detected using SP-LIBS

Received 12 October 2006; accepted 20 November 2006.
* Author to whom correspondence should be sent. E-mail: angel@mail.chem.sc.edu.

0003-7028/07/6102-0171$2.00/0

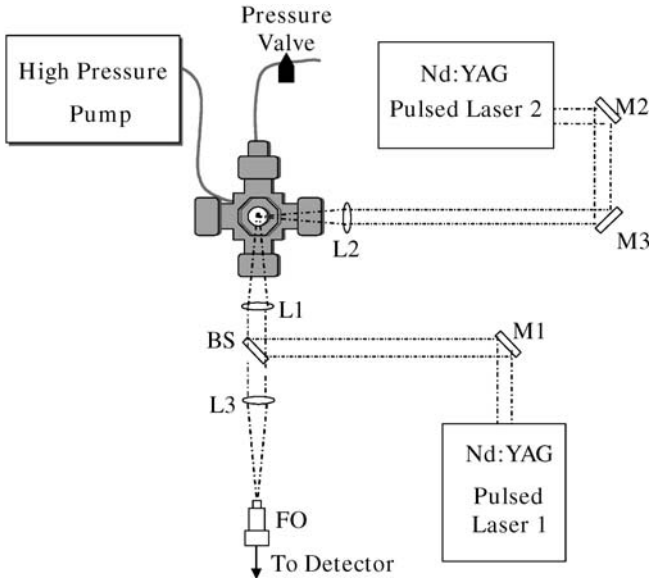

FIG. 1. Schematic diagram of DP-LIBS apparatus. The labels L, M, BS, and FO indicate lenses, mirrors, the beamsplitter, and the fiber optic, respectively.

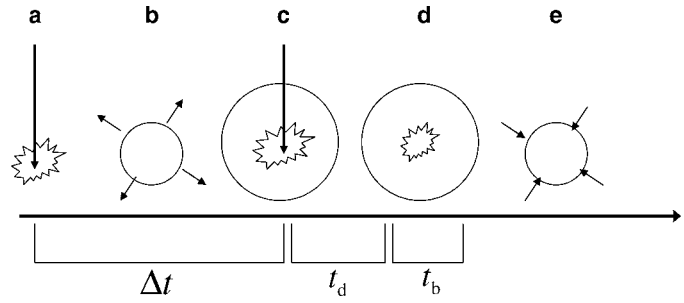

FIG. 2. Schematic of DP-LIBS timing parameters. (**a**) First laser pulse, E_1, forms the initial LIP in bulk solution; (**b**) laser-induced breakdown and heating of the solution by the first LIP forms an expanding laser-induced vapor bubble; (**c**) second laser pulse, E_2, forms the second LIP inside the laser-induced bubble environment; (**d**) DP-LIBS emission is collected; (**e**) bubble shrinks and collapses. The timing parameters, Δt, t_d, and t_b are defined as the time interval between the two laser pulses, steps (a) and (c), the interval between E_2 (c) and emission collection (d), and the interval over which the DP-LIBS emission is integrated (d), respectively. For SP-LIBS, analyte emission would be collected directly following formation of the first LIP (a).

while hydrogen, oxygen, and elements with emission originating at higher energy levels (such as zinc) were virtually undetectable. In this paper, we extend our previous SP-LIBS work to include DP-LIBS of high-pressure bulk aqueous solution. This work is performed in hopes of expanding the range of elements that can be detected at pressures corresponding to those of the deep ocean and to ultimately determine the suitability of LIBS for *in situ* analysis of hydrothermal vent fluids.

EXPERIMENTAL

Spectral Measurements. The basic DP-LIBS experimental setup is shown in Fig. 1. Two Nd:YAG laser pulses (Continuum Surelite III, 5 ns pulse, and Quantel Nd 580 laser, 9 ns pulse; 1064 nm; 5 Hz) were focused into a high-pressure sample chamber constructed of stainless steel Swagelok fittings (Central Swagelok Company, Solon, OH). The high-pressure chamber was described previously.[31] Ten centimeter (10 cm) focal-length fused silica lenses were used to focus the laser pulses and to collect and focus plasma emission onto the collection optical fiber. All optics were mounted on micrometer stages, allowing precise control of beam overlap and collection field of view within the high-pressure cell. The LIP emission was collected collinear with the path of the first laser pulse to ensure optimal overlap between the collection field of view and the laser-induced vapor cavity. We utilized an orthogonal configuration for the second laser pulse rather than a collinear configuration, based on our previous investigations, which indicated that an orthogonal pulse geometry allows more precise control of LIP alignment and thereby yields higher signal enhancements for several dissolved species in bulk aqueous solution.[41] The energies of the two laser pulses were held constant at 30 and 200 mJ/pulse for the first 9-ns and second 7-ns laser pulse, respectively, and were measured as the energy incident on the lenses (L_1 and L_2 in Fig. 1) used to focus the laser pulses into the sample chamber. The e-folding scale (i.e., the distance over which the field attenuates by 1/e) for pure water at 1064 nm is about 2.2 cm, and therefore at the laser focus (3 cm into the bulk solution) about 76% of the laser energy (including reflection losses) incident on the focusing lens is attenuated. Therefore, the effective pulse energies, E_1 and E_2, were approximately 7 and 48 mJ/pulse, respectively. The pulse energies were not optimized as part of this study, but were selected because they provided relatively intense and reproducible DP-LIBS emission.

A Chromex spectrograph (Model 250IS/RF, 0.25 m, *f*/4) was used with either a 300 grooves/mm grating (blazed at 1 μm, 0.5 nm spectral resolution) or a 1200 grooves/mm grating (blazed at 500 nm, 0.125 nm spectral resolution), both with a 50 μm slit width, coupled to a 2 mm core diameter, 0.51 NA light guide (Edmund Scientific Co. Model O2551), and an intensified charge-coupled device (ICCD) camera (Princeton Instruments I-Max 1024E), controlled with WinSpec/32 version 2.5.7.3 software. Detector gating was controlled using a pulse-timing generator (Roper Scientific ST-133A) coupled to the variable clock (Stanford Instruments Model SR250) and delay generator (Stanford Instruments Model DG535) used to control laser firing. Figure 2 defines important DP-LIBS timing parameters in relation to laser-induced bubble dynamics: the inter-pulse delay (Δt, the time interval between the two sequential laser pulses), the detector gate delay (t_d, the interval between the second laser pulse and collection of plasma emission), and the detector gate width (t_b, the duration of plasma emission integration).

All sample solutions were prepared using sodium and zinc bromide salts dissolved in deionized water and diluted to 1000 parts per million (ppm wt/vol). These concentrations were chosen to provide relatively intense analyte emission while avoiding detector saturation. Spectra were averaged over five replicate measurements, each the sum of 200 accumulations (i.e., 200 pulse pairs). Analyte emission intensities were calculated after baseline subtraction.

RESULTS

To the best of our knowledge, we are the first group to investigate LIBS for analysis of bulk solutions at elevated pressures.[31,55] Therefore, an important goal of these investigations is to determine pressure effects on DP-LIBS enhancements. With this knowledge we hope to demonstrate the

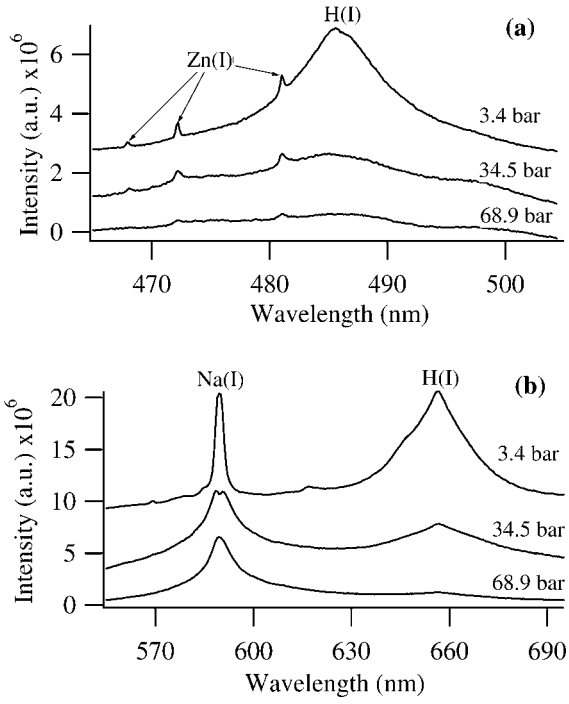

FIG. 3. Comparison of DP-LIBS emission spectra for a solution containing 1000 ppm Zn and Na at three different pressures, 3.4 bar, 34.5 bar, and 68.9 bar. (**a**) The 465–505 nm spectral region acquired using the 1200 grooves/mm grating. Upper trace (3.4 bar, $\Delta t = 48$ μs, $t_d = 300$ ns), middle trace (34.5 bar, $\Delta t = 10$ μs, $t_d = 200$ ns), and lower trace (68.9 bar, $\Delta t = 6$ μs, $t_d = 140$ ns); $t_b = 200$ ns. The Zn(I) lines (468.014, 472.215, and 481.053 nm) and the broad H_β spectral feature (486.1 nm) are labeled. (**b**) The 565–695 nm spectral region acquired using the 300 grooves/mm grating. Upper trace (3.4 bar, $\Delta t = 48$ μs, $t_d = 300$ ns), middle trace (34.5 bar, $\Delta t = 5$ μs, $t_d = 200$ ns), and lower trace (68.9 bar, $\Delta t = 1.5$ μs, $t_d = 140$ ns); $t_b = 1$ μs. The Na(I) doublet (588.995 and 589.592 nm) and the broad H_α spectral feature (656.3 nm) are labeled. $E_1 = 7$ mJ/pulse and $E_2 = 48$ mJ/pulse. All spectra were measured using conditions determined as part of brief optimization studies. The upper traces are offset for clarity.

feasibility and determine the limitations of DP-LIBS for measuring dissolved analytes in the deep ocean.

Figure 3 shows DP-LIBS emission spectra for a solution containing Zn and Na for three different pressures, 3.4 bar, 34.5 bar, and 68.9 bar (1 bar = 101.325 kPa and corresponds to ~10 meters ocean depth), over two different spectral regions (465–505 nm, Fig. 3a, and 560–695 nm, Fig. 3b). Zinc and hydrogen emission were used to indicate DP-LIBS enhancements (both elements were only observed using DP-LIBS as opposed to SP-LIBS), and sodium emission (which is easily observed using SP-LIBS) was used to compare SP- and DP-LIBS emission behavior. The spectra shown in Figs. 3a and 3b were acquired using the optimal detector and laser timing values that provided the maximum Zn(I) and Na(I) emission intensity, respectively, at each pressure.

It should be noted that the limited spectral resolution of the system (~0.5 nm) prevented the Na(I) doublet (588.995 and 589.592 nm) from being resolved even at the lowest pressure investigated (3.4 bar).

The spectra shown in Fig. 3 reveal that the DP-LIBS emission intensities and line widths strongly depend on solution pressure. We observed that as the pressure is increased the DP-LIBS emission intensity decreases rapidly such that only minimal DP-LIBS enhancement (and, thus, little or no H_α, H_β, or Zn(I) emission) was observed at pressures exceeding ~100 bar (spectra not shown). On the other hand, Na(I) emission (which was easily observed using SP-LIBS at pressures exceeding 275 bar)[31] could be observed for all pressures investigated. It is not known whether ~100 bar represents a general maximum pressure limit for DP-LIBS analysis of high-pressure bulk solution or if the limit is due to the specific experimental parameters used in these studies. However, these findings are in agreement with previous work performed by Casavola et al.,[49] in which the maximum internal vapor pressure of the early-stage bubble was calculated to be on the order of 100 bar. It is reasonable that if the solution pressure is greater than or equal to the initial pressure inside the bubble (~100 bar), then this greater external pressure exerted on the bubble would force the bubble to collapse almost instantly, eliminating the bubble that leads to DP-LIBS enhancement.

The small dip in the Na(I) emission spectrum at 589 nm, shown for 34.5 bar (see Fig. 3b), is most likely a result of self-absorption, which may be attributed to the shorter inter-pulse delay value that was used ($\Delta t = 5$ μs for 34.5 versus 48 μs for 3.4 bar). This is in agreement with previous work that shows that self-absorption (following excitation with the second LIP) is more likely to be observed during the early stages of laser-induced bubble evolution (shorter Δt values) and becomes less pronounced as the bubble expands and the vapor density inside the laser-induced bubble decreases.[43] However, self-absorption effects were not apparent when Δt was further decreased to 1.5 μs (for 68.9 bar). We are currently investigating the reasons for this observation, but it is possible that additional line broadening (caused by the higher densities and temperatures present inside the bubble at an even earlier stage) prevented any effects of self-absorption from being resolved.

In a previous report,[53] even moderately low water pressures (up to 5 bar) have been shown to affect laser-induced bubble dynamics, for example, the maximum bubble size and bubble lifetime both decrease with increasing solution pressure. It is reasonable then, that pressure effects on the laser-induced bubble lead to the observed decrease in DP-LIBS emission intensity with increasing pressure (see Fig. 3), because the internal conditions of the dynamic laser-induced vapor bubble (i.e., the bubble volume and the temperature and pressure inside the bubble) would have a strong influence on the LIP produced inside the bubble by the second laser pulse. Our investigations of DP-LIBS emission enhancements for several elements (Zn, H, and Na) over a range of inter-pulse delays ($0 < \Delta t \leq 400$ μs) and solution pressures (up to 137.9 bar) not only allowed selection of suitable bubble conditions for excitation by the second LIP (thereby optimizing the resulting DP-LIBS emission enhancements), but also made it possible to infer how solution pressure affects the laser-induced bubble dynamics.

Figure 4a shows Zn(I) DP-LIBS emission intensity versus Δt, from 0–80 μs for five different pressures (3.4 bar, 6.8 bar, 34.5 bar, 68.9 bar, and 137.9 bar). A relatively short gate delay ($t_d = 150$ ns) and long gate width ($t_b = 1$ μs) were used to ensure that the majority of the analyte emission was collected regardless of any pressure effects. The overall Zn(I) emission intensity measured for 3.4 bar cannot be directly compared to the intensities for the other four pressures due to a slight shift in optical focusing between experiments. For this reason, the intensity data for 3.4 bar is shown on a different scale (right axis) than the other four pressures (left axis). Figures 4b and 4c

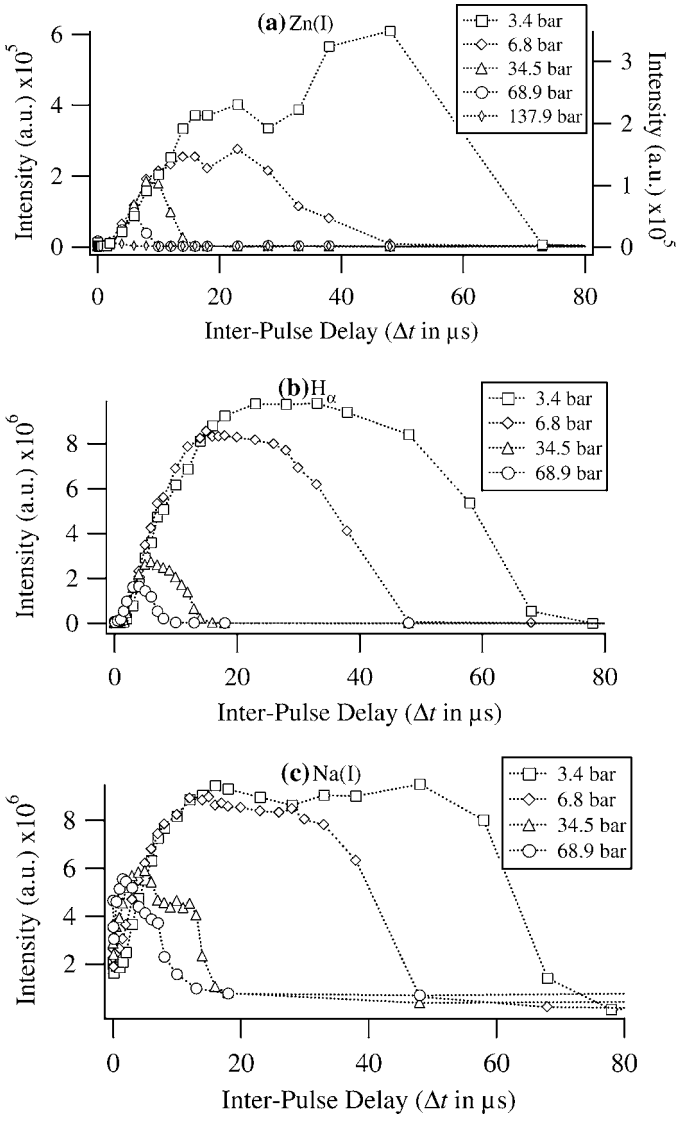

FIG. 4. DP-LIBS emission intensity of three different elements as a function of Δt (0–80 μs), for several different pressures. (**a**) Zn(I) emission (481.053 nm) intensity for 6.8 bar, 34.5 bar, 68.9 bar, and 137.9 bar (left axis), and 3.4 bar (right axis); $t_d = 150$ ns; grating = 1200 grooves/mm; (**b**) H_α emission (656.3 nm), and (**c**) Na(I) doublet emission (588.995 and 589.592 nm) intensity, for 3.4 bar ($t_d = 300$ ns), 6.8 bar ($t_d = 250$ ns), 34.5 bar ($t_d = 200$ ns), and 68.9 bar ($t_d = 140$ ns); grating = 300 grooves/mm. For all measurements, $E_1 = 7$ mJ/pulse and $E_2 = 48$ mJ/pulse; $t_b = 1$ μs. Data points and error bars are not shown for the sake of clarity (RSD ≈ 10%).

show the DP-LIBS emission intensity of the H_α line at 656 nm and the unresolved Na(I) doublet (588.995 and 589.592 nm), respectively, for Δt ranging from 0 to 80 μs and pressures between 3.4 and 68.9 bar. The large spectral window (~80 nm with the 300 grooves/mm grating) allowed H_α and Na(I) emission signals to be measured simultaneously. Gate delays of 300, 250, 200, and 140 ns were used for 3.4, 6.8, 34.5, and 68.9 bar, respectively, and t_b was constant at 1 μs. These timing parameters were chosen based on brief optimization studies to provide the maximum emission for each of the pressures investigated.

As expected, the data shown in Fig. 4 reveal that when the two laser pulses arrive at approximately the same time ($\Delta t = 0$ μs), the experiment is essentially SP-LIBS in nature (i.e., no DP-LIBS enhancement is observed). As Δt is increased, however, the resulting DP-LIBS emission intensity increases rapidly before leveling off and falling back to the SP-LIBS levels. Not surprisingly, then, the Na(I) emission (which has lower energy excited states and is easily observed using SP-LIBS) was observed for all Δt values (see Fig. 4c), while Zn(I) and H_α emission (having higher energy excited states) were only detected over a limited range of Δt values (see Figs. 4a and 4b, respectively). Additionally, as previously discussed, when the solution pressure was increased to 137.9 bar, very little Zn(I) (see Fig. 4a) or H_α emission (data not shown) was observed using any of the Δt values investigated.

Assuming a single spherical laser-induced bubble, the initial rise in DP-LIBS emission intensity with increasing Δt (as shown in Fig. 4) is most likely related to the increasing bubble volume into which the LIP can expand, as maximal (or minimally hindered) expansion of the second LIP should produce more intense and longer-lasting plasma emission. The larger bubble volume should also reduce the effects of plasma quenching at the vapor–water interface by reducing the plasma's surface-to-volume ratio and, therefore, producing greater analyte emission.[37] Additionally, as the bubble expands (as the laser-induced bubble volume increases), there is an increased possibility that the second LIP completely overlaps the laser-induced bubble, thereby limiting partial breakdown of the water surrounding the bubble (and the fraction of energy that goes into vaporization) and increasing the observed DP-LIBS emission. Previous investigations have also shown that the optimal DP-LIBS atomic emission intensity is achieved when the second LIP is formed around the time of the maximum expansion of the laser-induced bubble.[34,49,52] The fall-off of DP-LIBS intensity following the maximum emission region is most likely related to bubble compression and collapse, which leads to faster cooling of the plasma and shorter emission lifetimes and intensities.[49,52] It is interesting to note that during bubble collapse we see little evidence of additional bubble oscillations (i.e., oscillations in DP-LIBS emission intensity in Figs. 4a–4c), although this may simply be attributed to the low temporal resolution of our experiments.

In general, we see that, for all solution pressures, the DP-LIBS emission intensity initially increases with Δt at a similar rate. However, the maximum emission intensity, the range of Δt values providing significant enhancement, and the point at which the maximum DP-LIBS enhancement is observed (Δt_{opt}) all decrease rapidly with increasing solution pressure. The maximum 481.053 nm Zn(I) emission intensity, for example, was observed for Δt_{opt} of 48, 23, 10, 6, and 2 μs for pressures of 3.4, 6.8, 34.5, 68.9, and 137.9 bar, respectively (see Fig. 4a). The slopes of the curves shown in Fig. 4 indicate that the vapor bubble initially expands at a rate independent of the external pressure. This is to be expected since the initial pressure inside the bubble should be higher than the external pressure. However, as the vapor pressure inside the bubble begins to approach the external solution pressure, the rate of expansion slows and levels off, eventually leading to bubble collapse. For higher solution pressures, the expanding bubble is overcome by the increased external pressure at earlier points in the bubble evolution, thus leading to earlier bubble collapse and a corresponding decrease in the bubble lifetimes; this is consistent with the observation that at higher pressures, the bubble does not have time to expand to the maximum size achieved in lower pressure solutions.[53]

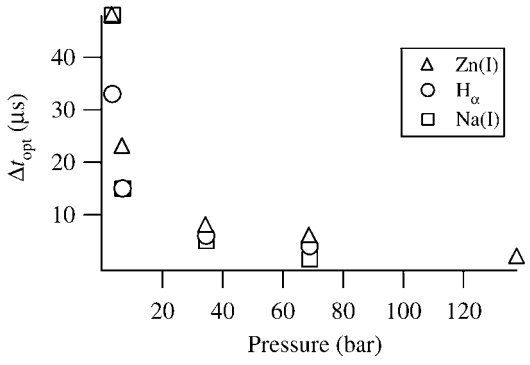

FIG. 5. Pressure dependence of the optimal inter-pulse delay, Δt_{opt}, for Zn(I) (481.053 nm), H_α, and Na(I) (588.995 and 589.592 nm) DP-LIBS emission.

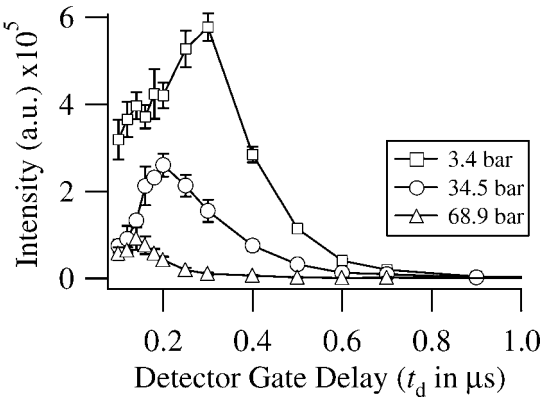

FIG. 6. Temporal dependence of 481.053 nm Zn(I) DP-LIBS emission intensity for 3.4 bar, 34.5 bar, and 68.9 bar. Measurements were made using Δt values of 48, 10, and 6 μs, for the three pressures, respectively; $E_1 = 7$ mJ/pulse and $E_2 = 48$ mJ/pulse; $t_b = 200$ ns; grating = 1200 grooves/mm (error bars represent 1σ).

Using the Zn(I), H_α, and Na(I) data shown in Fig. 4, the pressure dependency of the optimal inter-pulse delay, Δt_{opt}, was plotted and is shown in Fig. 5 for all three elements. Figure 5 indicates that as the solution pressure is increased the maximum DP-LIBS emission is achieved at increasingly shorter Δt values (Δt_{opt}). Given the discussion above, if the second LIP is focused inside the bubble following shorter Δt delays, as required for achieving maximum DP-LIBS enhancements at elevated pressures ($\Delta t_{opt} = 10$ and 6 μs for pressures of 34.5 and 68.9 bar, respectively), the bubble is given less time to expand and cool before arrival of the second laser pulse, and thus the expanding LIP should be confined and quenched to a greater extent. This is shown in Fig. 6, which shows the temporal evolution ($0.08 \leq t_d \leq 1$ μs) of Zn(I) DP-LIBS emission intensity measured using the previously determined Δt_{opt} values of 48, 10, and 6 μs for solution pressures of 3.4 bar, 34.5 bar, and 68.9 bar, respectively ($t_b = 200$ ns). As expected, the increased confinement at shorter Δt values results in faster plasma cooling (i.e., shorter emission lifetimes) and lower overall DP-LIBS emission signals, as shown for the higher pressure data (34.5 and 68.9 bar) in Fig. 6.

In discussing the experimental results reported herein, we assumed a single spherical laser-induced bubble shape for the entire laser-induced bubble lifetime. However, the sphericity of bubbles produced during these investigations is not known, due to the fact that we were not set up for bubble imaging at the time that the measurements were made. On the other hand, recent bubble images taken in our lab show that, due to the conical shape of the focal volume and multiple breakdown sites along the beam waist, the first LIP may produce many small bubbles that coalesce to form elongated ellipsoidal-shaped bubbles, as opposed to a single spherical bubble. We observe that the deviation from a spherical shape decreases with decreasing laser fluence, and because the investigations reported herein utilized a low laser pulse energy of about 7 mJ/pulse, the deviation should be minimal. Additionally, a previous investigation[56] using similar excitation conditions (30 mJ, 8 ns, 1064 nm Nd:YAG laser pulses, $f = 25.4$ mm) showed the formation of single spherical bubbles. Although it is possible that an aspherical bubble, as opposed to a spherical bubble, was interrogated with the second LIP, the interpretations of our observations should still hold.

In summary, ambient solution pressure appears to have a significant effect on laser-induced bubble dynamics and a corresponding effect on DP-LIBS enhancements. As solution pressure increases, the bubble lifetime and DP-LIBS enhancements decrease to the point that little, or no, enhancements are observed above ~100 bar. Based on these observations, it appears that the range of solution pressures over which DP-LIBS provides enhancement is limited by the decreased laser-induced bubble lifetime at elevated pressures. It may be possible to increase the bubble lifetime at high pressures by increasing the laser-induced bubble radius, bubble energy, and/or conversion efficiency of laser energy to bubble energy. Previous investigations have shown that these bubble parameters strongly depend on several laser excitation parameters including pulse duration, pulse energy, laser wavelength, and focusing optics.[32,37,53,57] It may also be possible to extend the bubble lifetime by re-expanding the bubble with a second laser pulse, followed by analysis with a third laser pulse. We are currently investigating whether or not different excitation parameters can be used to extend bubble lifetimes and DP-LIBS enhancements at elevated pressures.

CONCLUSION

We have investigated sequential-pulse LIBS for analysis of high-pressure solutions in an attempt to increase the sensitivity of LIBS for potential application to deep-ocean analysis. Our investigations reveal that increasing solution pressure reduces DP-LIBS emission enhancements, and that as the solution pressure is increased above approximately 100 bar, the DP-LIBS emission enhancements decrease to the point that little or no DP-LIBS emission is observed. DP-LIBS spectral features (specifically, emission intensity and line width) are significantly affected by solution pressure, and these observed pressure effects depend on experimental parameters associated with bubble expansion and collapse (including the delay between the two laser pulses and the time at which emission is observed following the laser pulse).

These results are in contrast to our previous investigations using SP-LIBS,[31,55] in which pressure was shown to have only minor effects on SP-LIBS emission. The differences between SP- and DP-LIBS analyte emission behavior with increasing solution pressure seems to be related to the fact that the SP-LIBS plasma is formed in a static liquid environment while the DP-LIBS plasma is formed in a dynamic bubble environment that is significantly influenced by solution pressure. As the laser-induced bubble expands, it appears that the elevated solution pressure confines the expanding bubble, causing the

bubble to collapse earlier (decreasing the bubble lifetime). As a result, the smaller, shorter-lived bubble never reaches the conditions that provide the large DP-LIBS enhancements seen for low-pressure solutions.

Future investigations will determine whether different experimental conditions (i.e., laser wavelength, energy density, pulse duration, and focusing optics, or additional laser pulses) can be used to extend the bubble lifetime and thereby extend DP-LIBS' applicability to higher pressures. We will also utilize direct spectral imaging of the laser-induced plasma and bubble for a range of solution pressures to gain additional insight into the effects of pressure on plasma and bubble dynamics. Our ongoing LIP and bubble imaging studies will help reveal how bubble shape and dynamics, as well as overlap between the laser-induced bubble and the second LIP, define emission intensities, linewidths, LIP lifetimes, and other DP-LIBS measurements. Preliminary LIBS investigations of solid samples in high-pressure solutions are also underway.

ACKNOWLEDGMENTS

We would like to thank the National Science Foundation for support of this work under grant numbers OCE-0352242, OCE-0527927, OCE-0352278, and CHE-0316069.

1. F. Brech and L. Cross, Appl. Spectrosc. **16,** 59 (1962).
2. D. A. Cremers, Appl. Spectrosc. **41,** 572 (1987).
3. C. M. Davies, H. H. Telle, D. J. Montgomery, and R. E. Corbett, Spectrochim. Acta, Part B **50,** 1059 (1995).
4. B. J. Marquardt, S. R. Goode, and S. M. Angel, Anal. Chem. **68,** 977 (1996).
5. B. J. Marquardt, D. N. Stratis, D. A. Cremers, and S. M. Angel, Appl. Spectrosc. **52,** 1148 (1998).
6. O. Samek, D. C. S. Beddows, J. Kaiser, S. V. Kukhlevsky, M. Liška, H. H. Telle, and J. Young, Opt. Eng. **39,** 2248 (2000).
7. H. H. Telle, D. C. S. Beddows, G. W. Morris, and O. Samek, Spectrochim. Acta, Part B **56,** 947 (2001).
8. S. Palanco, J. M. Baena, and J. J. Laserna, Spectrochim. Acta, Part B **57,** 591 (2002).
9. R. C. Wiens, S. K. Sharma, J. Thompson, A. Misra, and P. G. Lucey, Spectrochim. Acta, Part A **61,** 2324 (2005).
10. J. D. Blacic, D. R. Pettit, D. A. Cremers, and N. Roessler, "Laser-Induced Breakdown Spectroscopy for Remote Elemental Analysis of Planetary Surfaces", Proceedings of the International Symposium on Spectral Sensing Research, 302 (1992).
11. C. M. Davies, H. H. Telle, and A. W. Williams, Fresenius' J. Anal. Chem. **355,** 895 (1996).
12. X. D. Hou and B. T. Jones, Microchem. J. **66,** 115 (2000).
13. A. K. Knight, N. L. Scherbarth, D. A. Cremers, and M. J. Ferris, Appl. Spectrosc. **54,** 331 (2000).
14. J. Gruber, J. Heitz, H. Strasser, D. Bäuerle, and N. Ramaseder, Spectrochim. Acta, Part B **56,** 685 (2001).
15. A. I. Whitehouse, J. Young, I. M. Botheroyd, S. Lawson, C. P. Evans, and J. Wright, Spectrochim. Acta, Part B **56,** 821 (2001).
16. Z. A. Arp, D. A. Cremers, R. D. Harris, D. M. Oschwald, G. R. Parker, Jr., and D. M. Wayne, Spectrochim. Acta, Part B **59,** 987 (2004).
17. C. López-Moreno, S. Palanco, and J. J. Laserna, Spectrochim. Acta, Part B **60,** 1034 (2005).
18. B. Sallé, J.-L. Lacour, P. Mauchien, P. Fichet, S. Maurice, and G. Manhés, Spectrochim. Acta, Part B, paper in press (2006).
19. S. Palanco, C. López-Moreno, and J. J. Laserna, Spectrochim. Acta, Part B **61,** 88 (2006).
20. C. López-Moreno, S. Palanco, J. J. Laserna, F. DeLucia, Jr., A. W. Miziolek, J. Rose, R. A. Walters, and A. I. Whitehouse, J. Anal. At. Spectrom. **21,** 55 (2006).
21. L. Paksy, B. Német, A. Lengyel, L. Kozma, and J. Czekkel, Spectrochim. Acta, Part B **51,** 279 (1996).
22. M. Tran, Q. Sun, B. Smith, and J. D. Winefordner, Anal. Chim. Acta **419,** 153 (2000).
23. R. T. Wainner, R. S. Harmon, A. W. Miziolek, K. L. McNesby, and P. D. French, Spectrochim. Acta, Part B **56,** 777 (2001).
24. R. Barbini, F. Colao, V. Lazic, R. Fantoni, A. Palucci, and M. Angelone, Spectrochim. Acta, Part B **57,** 1203 (2002).
25. D. Bulajic, G. Cristoforetti, M. Corsi, M. Hidalgo, S. Legnaioli, V. Palleschi, A. Salvetti, E. Tognoni, S. Green, D. Bates, A. Steiger, J. Fonseca, J. Martins, J. McKay, B. Tozer, D. Wells, R. Wells, and M. A. Harith, Spectrochim. Acta, Part B **57,** 1181 (2002).
26. M. Noda, Y. Deguchi, S. Iwasaki, and N. Yoshikawa, Spectrochim. Acta, Part B **57,** 701 (2002).
27. W. B. Lee, J. Wu, Y. I. Lee, and J. Sneddon, Appl. Spectrosc. **39,** 27 (2004).
28. C. A. Munson, F. C. DeLucia, Jr., T. Piehler, K. L. McNesby, and A. W. Miziolek, Spectrochim. Acta, Part B **60,** 1217 (2005).
29. B. Sallé, D. A. Cremers, S. Maurice, and R. C. Wiens, Spectrochim. Acta, Part B **60,** 479 (2005).
30. L. Radziemski, D. A. Cremers, K. Benelli, C. Khoo, and R. D. Harris, Spectrochim. Acta, Part B **60,** 237 (2005).
31. M. Lawrence-Snyder, J. Scaffidi, S. M. Angel, A. P. M. Michel, and A. D. Chave, Appl. Spectrosc. **61,** 786 (2006).
32. P. K. Kennedy, D. X. Hammer, and B. A. Rockwell, Prog. Quant. Electr. **21(3),** 155 (1997).
33. Y.-I. Lee, K. Song, and J. Sneddon, *Laser-Induced Breakdown Spectroscopy* (Nova Science, New York, 2000), Chap. 3.
34. S. Koch, R. Court, W. Garen, W. Neu, and R. Reuter, Spectrochim. Acta, Part B **60,** 1230 (2005).
35. D. A. Cremers, L. J. Radziemski, and T. R. Loree, Appl. Spectrosc. **38,** 721 (1984).
36. R. Nyga and W. Neu, Opt. Lett. **18,** 747 (1993).
37. A. E. Pichahchy, D. A. Cremers, and M. J. Ferris, Spectrochim. Acta, Part B **52,** 25 (1997).
38. R. Knopp, F. J. Scherbaum, and J. I. Kim, Fresenius' J. Anal. Chem. **355,** 16 (1996).
39. D. C. S. Beddows, O. Samek, M. Liska, and H. H. Telle, Spectrochim. Acta, Part B **57,** 1461 (2002).
40. W. F. Pearman, J. Scaffidi, and S. M. Angel, "Trace Metal Analysis in Bulk Aqueous Solution Using Nanosecond Dual Pulse Laser Induced Breakdown Spectroscopy", in *Trends in Optics and Photonics Book Series* (Optical Society of America, 2002), Book 81 (*Laser Induced Plasma Spectroscopy and Applications*), p. 218.
41. W. Pearman, J. Scaffidi, and S. M. Angel, Appl. Opt. **42,** 6085 (2003).
42. S. Koch, W. Garen, M. Müller, and W. Neu, Appl. Phys. A **79,** 1071 (2004).
43. L. St-Onge, E. Kwong, M. Sabsabi, and E. B. Vadas, J. Pharm. Biomed. Anal. **36,** 277 (2004).
44. A. De Giacomo, M. Dell'Aglio, F. Colao, and R. Fantoni, Spectrochim. Acta, Part B **59,** 1431 (2004).
45. A. De Giacomo, M. Dell'Aglio, and O. De Pascale, Appl. Phys. A **79,** 1035 (2004).
46. V. Lazic, F. Colao, R. Fantoni, and V. Spizzicchino, Spectrochim. Acta, Part B **60,** 1014 (2005).
47. A. De Giacomo, M. Dell'Aglio, F. Colao, R. Fantoni, and V. Lazic, Appl. Surf. Sci. **247,** 157 (2005).
48. V. Lazic, F. Colao, R. Fantoni, and V. Spizzicchino, Spectrochim. Acta, Part B **60,** 1002 (2005).
49. A. Casavola, A. De Giacomo, M. Dell'Aglio, F. Taccogna, G. Colonna, O. De Pascale, and S. Longo, Spectrochim. Acta, Part B **60,** 975 (2005).
50. L. J. Radziemski, T. R. Loree, D. A. Cremers, and N. M. Hoffman, Anal. Chem. **55,** 1246 (1983).
51. X. Mao, X. Zeng, S. B. Wen, and R. E. Russo, Spectrochim. Acta, Part B **60,** 960 (2005).
52. A. De Giacomo, M. Dell'Aglio, A. Casavola, G. Colonna, O. De Pascale, and M. Capitelli, Anal. Bioanal. Chem. **385,** 303 (2006).
53. B. Wolfrum, T. Kurz, O. Lindau, and W. Lauterborn, Phys. Rev. E **64,,** 046306-1 (2001).
54. M. Hosoda, S. Aoshima, T. Itoh, and Y. Tsuchiya, Jpn. J. Appl. Phys. **38,** 3567 (1999).
55. A. P. M. Michel, M. Lawrence-Snyder, S. M. Angel, and A. D. Chave, Appl. Opt., paper submitted (2006).
56. C.-D. Ohl, Phys. Fluids **14,** 2700 (2002).
57. J. Noack, D. X. Hammer, G. D. Noojin, B. A. Rockwell, and A. Vogel, J. Appl. Phys. **83,** 7488 (1998).